ACS Macro Letters

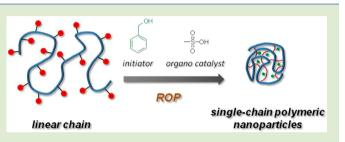
Biocompatible Single-Chain Polymeric Nanoparticles via Organo-Catalyzed Ring-Opening Polymerization

Edgar H. H. Wong, Shu Jie Lam, Eunhyung Nam, and Greg G. Qiao*

Department of Chemical and Biomolecular Engineering, The University of Melbourne, Parkville, Victoria 3010, Australia

Supporting Information

ABSTRACT: This study presents a novel approach to synthesize biocompatible single-chain polymeric nanoparticles (SCPN) under mild reaction conditions via organo-catalyzed ring-opening polymerization (ROP). Linear polymeric precursors containing pendent polymerizable caprolactone groups, made by reversible addition—fragmentation chain transfer (RAFT) polymerization, were intramolecularly crosslinked via ROP in the presence of benzyl alcohol (nucleophilic initiator) and methanesulfonic acid (organo catalyst) to form

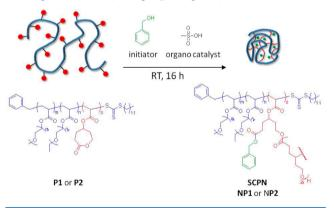


discrete, well-defined SCPN, as confirmed by GPC, DLS, ¹H NMR, and AFM analysis. The formed SCPN are tunable in size (2-5 nm), depending on the molecular weight of the parent linear macromolecule. Furthermore, cytotoxicity studies revealed that the SCPN, which were covalently cross-linked by biodegradable polyester linkages, were nontoxic toward human embryonic kidney (HEK293T) cells. This study demonstrates the efficiency and versatility of this approach to generate uniformly sized soft nanoparticles with tunable dimensions that are potentially useful for a range of targeted applications, including drug delivery systems and membranes for gas separation technologies.

The development of functional polymeric nanoparticles in the sub-20 nm size regime has been a subject of great scientific interest in recent years because of their potential applications in controlled drug delivery,^{1,2} bioimaging,^{3,4} catalysis,⁵ and substrate templating.⁶ Various techniques were developed for the preparation of such polymeric nanoparticles within this size regime, including the arm-first approach synthesis of core cross-linked star polymers using controlled polymerization protocols.⁷⁻¹⁰ In addition, emulsion-based systems have also been reported as viable options in the synthesis of soft nanoparticles.¹¹ Another well-known method in generating well-defined nanostructures entails the intra-molecular point-folding^{12,13} or cross-linking of collapsed single polymer chains via (dynamic) covalent or noncovalent interactions.^{6,14–28} This biomimetic approach, which was inspired by the self-folding of natural biomolecules,²⁹ has its advantages. For example, well-defined linear macromolecules with tailored functionalities and compositions can be preformed efficiently through modern synthetic polymer chemistry, thereby leading to precisely nanoengineered particles with narrow size distribution. Furthermore, this single-chain selfcross-linking approach enables the formation of nanoparticles as small as 5 nm, which is difficult to achieve with other methods, and can have potential applications for drug delivery across the blood-brain barrier.^{2,30}

Herein, we report a new synthetic approach in forming single-chain polymeric nanoparticles (SCPN) by intramolecular cross-linking of linear polymer chains bearing pendant lactone moieties via organo-catalyzed ring-opening polymerization $(ROP)^{31,32}$ (Scheme 1). Utilizing the versatility and efficiency of organo-catalyzed ROP, the current approach not only allows

Scheme 1. Collapse of Single Polymer Chains to Form Monodisperse Nanoparticles via Intramolecular Cross-Linking Mediated by Ring-Opening Polymerization



the formation of SCPN under metal-free and mild reaction conditions (i.e., at ambient temperature and moderate reaction times), but also the generation of biocompatible and biodegradable linkages (e.g., polyester) that stabilize the SCPN. Moreover, additional functional groups can be facilely introduced into the SCPN structure through the initiator employed in the ROP cross-linking step. Specifically, linear random copolymers of oligo(ethylene glycol) methyl ether acrylate, di(ethylene glycol) ethyl ether acrylate and 4-

Received: April 13, 2014 Accepted: May 14, 2014 Published: May 19, 2014

ACS Macro Letters

(acryloyloxy)-*ɛ*-caprolactone³³ were made via reversible addition–fragmentation chain transfer (RAFT)³⁴ polymerization, followed by SCPN formation via ROP in the presence of a nucleophilic initiator (benzyl alcohol) and organo catalyst (methanesulfonic acid). The formed SCPN were characterized thoroughly by gel-permeation chromatography (GPC), dynamic light scattering (DLS), proton nuclear magnetic resonance (¹H NMR) spectroscopy and atomic force microscopy (AFM) in the dry state. The biocompatibility of the resulting SCPN was then assessed via colorimetric assay with human embryonic kidney (HEK293T) cells.

In general, RAFT was chosen as the polymerization method of choice to make different molecular weights of the desired linear random copolymer precursors **P1** and **P2** (poly[(oligo-(ethylene glycol) methyl ether acrylate)-*ran*-(di(ethylene glycol) ethyl ether acrylate)-*ran*-(4-(acryloyloxy)- ε -caprolactone)]) as a result of the ability of this technique to mediate radical polymerizations at moderate reaction temperatures (<100 °C) and in the absence of metal/ligand catalytic systems that may compromise the lactone functionality. In addition, ethylene glycol-based monomers were selected because of their biocompatibility and excellent solubility in both organic and aqueous solutions.

For the synthesis of P1 and P2 via RAFT polymerization, the reaction proceeded at 80 °C for 15 h during which about 93% monomer conversion was attained in both cases, as deduced from ¹H NMR analysis. In essence, both P1 and P2 have close to the targeted degree of polymerization of 200 and 100 repeat units, respectively, based on their calculated monomer conversions. The polymerizations were well-controlled as the GPC differential refractive index (DRI) chromatograms of both polymers, shown in Figure 1a,c, were monomodal and have low dispersity (D) values (D < 1.4), while ¹H NMR analysis indicated the successful incorporation of pendent lactone moieties into the polymer chains as resonances corresponding to the protons of the methanetriyl and methylene groups of the caprolactones (Figure 1e, resonances a and b, $\delta_{\rm H}$ 4.90–5.10 and 4.30-4.50 ppm, respectively) were clearly visible. The numberaverage molecular weight (M_n) and D values of both polymers, as determined by GPC using polystyrene standards, are listed in Table 1. Additionally, both P1 and P2 have on average about 19 mol % of lactone moieties per polymer chain, which is close to the targeted value of 20%.

The formation of SCPN NP1 and NP2 from P1 and P2, respectively, occurred at ambient temperature in the presence of benzyl alcohol and methanesulfonic acid in chloroform (affording an initiator-to-catalyst-to-lactone molar ratio of 1:2:7.3 and a total lactone concentration of 73 mM). Based on the NMR spectroscopic analysis of NP1 after 16 h of ROP, resonance b quantitatively shifted from $\delta_{\rm H}$ 4.30–4.50 to 4.00– 4.28 ppm, overlapping with the methylene protons from other ester groups, whereas new resonances d and e that correspond to the protons of the benzyl and hydroxyl groups appear at $\delta_{\rm H}$ 5.05 and 4.50-4.65 ppm, respectively (Figure 1e,f). In addition, the broadening of resonance a' was also observed after ROP. Similar observations were made for NP2. Beyond any doubt, the ¹H NMR results confirmed the ring-opening of caprolactones. GPC DRI chromatograms of NP1 and NP2 were compared to their linear precursors (Figure 1a,c). Both SCPN have smaller hydrodynamic volumes compared to their linear precursors as the GPC DRI chromatograms shifted from lower to higher retention times, which is exactly what one would expect to observe when a single polymer chain collapses

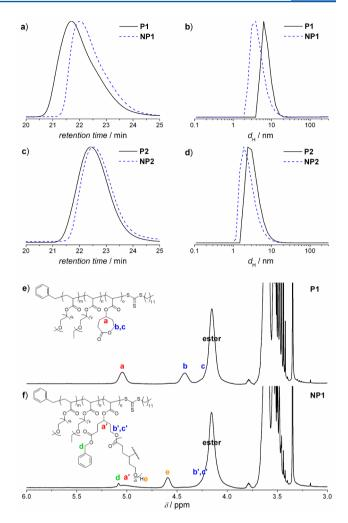


Figure 1. (a, c) GPC DRI chromatograms of the polymer precursors P1 and P2 as well as the corresponding single-chain polymeric nanoparticles NP1 and NP2, respectively. (b, d) DLS normalized mass ratio of linear polymer precursors (P1 and P2) and the formed nanoparticles (NP1 and NP2, respectively) as a function of hydrodynamic diameter ($d_{\rm H}$). ¹H NMR spectra of P1 before (e) and after (f) single-chain cross-linking via organo-catalyzed ring-opening polymerization: resonances that correspond to the key functional groups are labeled.

 Table 1. Characterization of Linear Polymer Precursors and Nanoparticles by GPC and DLS

sample	$M_{\rm n}~({\rm g}{\cdot}{\rm mol}^{-1})$	Đ	$d_{\rm H}~({\rm nm})$	% dispersity ^a
P1	49400	1.33	7.2	29
NP1	35600	1.64	4.8	51
P2	33200	1.15	3.6	52
NP2	29300	1.25	2.8	58
P3	27900	1.32	4.4	42
NP3	30100	1.76	5.0	41

"Measures the width of the peak obtained in DLS. This value is normalized to the mean size of the peak.

into a nanoparticle. The changes in M_n (which were measured based on the polymers' hydrodynamic volumes and not their exact molecular weights) were also apparent in both cases (Table 1). Further DLS analysis confirmed the trend observed in GPC as the formed **NP1** and **NP2** have smaller mean hydrodynamic diameter (d_H) values of 4.8 and 2.8 nm compared to 7.2 and 3.6 nm for P1 and P2, respectively (Figure 1b,d; Table 1). The fact that both P1 and P2 can form SCPN effectively suggests that our approach is versatile and the tuning of nanoparticle size can be achieved by simply varying the molecular weight of the linear polymer precursor.

AFM analysis was performed on **NP1** in order to obtain a visualization of the nanoparticle's morphology. Figure 2a shows

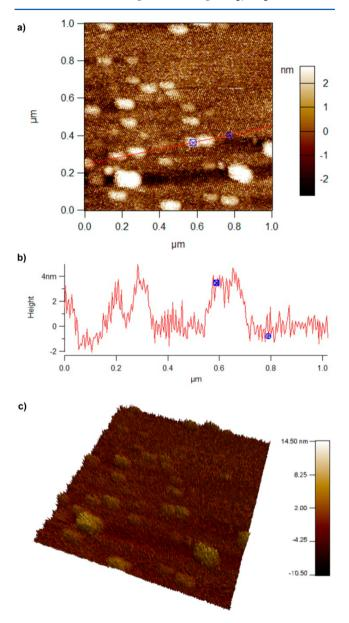


Figure 2. (a) AFM $(1 \times 1 \ \mu m)$ topography image of nanoparticles **NP1** casted on a polyethylenimine (PEI)-coated Si wafer. (b) The *z*-profile across the red line of the 2D AFM image in (a). (c) 3D height mode AFM $(1 \times 1 \ \mu m)$ image of the nanoparticles in (a).

the topography of diluted **NP1** solution $(1 \ \mu g \cdot mL^{-1}, 10 \ \mu L)$ in THF that was drop-casted onto a polyethylenimine-coated Si wafer, revealing distinct particulate entities that also include some larger aggregates. Closer inspection of the height profile in Figure 2b revealed **NP1** featuring an average height of about $4.3 \pm 0.3 \text{ nm}$, whereas statistical evaluation of all the particulate entities in Figure 2a yielded a mean height of 4.3 nm with a standard deviation of 1.6 nm (based on the plotted histogram in Figure S1a in the Supporting Information (SI)), which is in

close agreement to the $d_{\rm H}$ value of 4.8 nm as measured by DLS. No particles were observed for the P1 sample when subjected to AFM analysis (Figure S1b (SI)). Noteworthy, the particles were in their dried state, and as such it is not uncommon to form aggregates. Barner-Kowollik and co-workers have previously observed similar particle aggregates that could have formed during the casting process due to dewetting effects.²⁵ In addition, the nanoparticles' enhanced widths can also be caused by the broadness of the AFM tip.²⁵ Regardless, the AFM analysis in here serves as a very positive indicator in supporting the above-mentioned characterization data.

To prove that the formed SCPN was indeed as a result of cross-linking by ROP, an additional control experiment was performed where P1 was "reacted" in the abscence of methanesulfonic acid. After 16 h, the integrity of the caprolactone groups were preserved in the control sample based on ¹H NMR analysis. Additionally, the GPC DRI chromatograms of the control sample and P1 were identical, hence, validating the ROP approach in making SCPN. We have also synthesized a linear random copolymer precursor P3, which has the same chemical composition as P1 and P2 but with approximately double the amount of pendent caprolactones (ca. 40 mol %). P3 (with ca. 146 mM of caprolactone units) was subjected to the same ROP protocol using benzyl alcohol (10 mM) and methanesulfonic acid (20 mM) in chloroform to form NP3. ¹H NMR analysis yielded similar spectra to that obtained for NP1 and NP2, indicating the ringopening of caprolactones. However, a pronounced high molecular weight shoulder was observed in the GPC DRI chromatogram of NP3 that is most likely attributed to intermolecular cross-linked products between two or more polymer chains (Figure S2a (SI)). Based on DLS analysis (Figure S1b), NP3 has a bigger $d_{\rm H}$ compared to P3 (5.0 vs 4.4 nm). This suggests that increasing the concentration of lactone units will increase the probability of inter-over intramolecular reactions and, consequently, reduce the chances of forming well-defined SCPN. It is interesting to note that all ROP reactions were performed at a relatively high polymer concentration at about 100 mg·mL⁻¹ (i.e., 73 mM of lactone units for P1 and P2), which is at least 100 times more than the typical concentration reported in literature, yet no signs of gelation were observed. We have repeated the experiments at a lower polymer concentration at 20 mg·mL⁻¹ and obtained similar results. The exact reason as to why the formation of SCPN can occur at such high polymer concentrations in our approach is not entirely clear but we are in the process of performing structural and molecular simulations to further investigate this phenomenon. Nevertheless, the combination of GPC, ¹H NMR, DLS, and AFM analysis provided excellent evidence for the formation of SCPN via ROP at high polymer concentration.

Given that the formed SCPN in this study are water-soluble and consist of biocompatible ethylene glycol components, we therefore investigated the toxicity of **NP1** via a standard MTS assay that measures the metabolic activity of live cells in vitro. **NP1** was dissolved in sterile cell culture media at different concentrations (0, 2, 4, 8, 16, 32, 64, and 128 μ g·mL⁻¹) and incubated with human embryonic kidney cells (HEK293T), a model mammalian cell line. The UV absorbances of the cell culture mixture at λ = 490 nm after 24, 48, and 72 h were normalized to the positive growth control that consists of untreated cells. The cell viability was consistently high (>80%), regardless of the polymer-cell incubation time (Figure 3). In

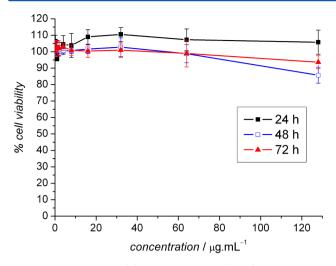


Figure 3. Percentage of living HEK293T cells after exposure to different concentrations of NP1.

addition, the increase in nanoparticle concentration (up to 128 μ g·mL⁻¹) did not appear to induce a significant decrease in cell viability. These findings demonstrate that **NP1** possess high biocompatibility.

In conclusion, we have demonstrated an efficient approach to generate SCPN via organo-catalyzed ROP-mediated intramolecular cross-linking of linear poly(oligo(ethylene glycol) acrylate) precursors containing pendent lactone moieties, as evidenced by GPC, DLS, ¹H NMR, and AFM analysis. The whole synthetic process excludes the use of any metal catalysts, thus, avoiding any potential toxic metal contamination. Moreover, SCPN of differing sizes can be precisely controlled by simply varying the molecular weight of the parent linear macromolecule. The formed SCPN in this study were also found to be biocompatible as they were nontoxic toward HEK293T cells. In addition, this approach enables the facile introduction of functional groups via the nucleophilic initiator, potentially allowing for further postmodification of the nanoparticles. Work is currently underway in our laboratories in employing these SCPN for drug delivery applications and gas separation technologies.

ASSOCIATED CONTENT

S Supporting Information

Detailed experimental and characterization procedures, as well as additional data. This material is available free of charge via the Internet at http://pubs.acs.org.

AUTHOR INFORMATION

Corresponding Author

*E-mail: gregghq@unimelb.edu.au.

Notes

The authors declare no competing financial interest.

ACKNOWLEDGMENTS

The authors acknowledge the Australian Research Council under the Future Fellowship (FT110100411, G.G.Q.) for financial support of this work. E.H.H.W. acknowledges the receipt of an Early Career Researcher Grant from The University of Melbourne.

Letter

REFERENCES

- (1) Dunn, S. S.; Byrne, J. D.; Perry, J. L.; Chen, K.; DeSimone, J. M. ACS Macro Lett. **2013**, *2*, 393–397.
- (2) Arruebo, M.; Fernandez-Pacheco, R.; Ibarra, M. R.; Santamaria, J. Nano Today **200**7, *2*, 22–32.
- (3) (a) Kim, B.; Schmeider, A. H.; Stacy, A. J.; Williams, T. A.; Pan, D. J. Am. Chem. Soc. **2012**, 134, 10377–10380. (b) Pan, D.; Cai, X.; Kim, B.; Stacy, A. J.; Wang, L. V.; Lanza, G. M. Adv. Healthcare Mater. **2012**, 1, 582–589.
- (4) Li, Y.; Liu, J.; Liu, B.; Tomczak, N. Nanoscale 2012, 4, 5694–5702.
- (5) Terashima, T.; Kamigaito, M.; Baek, K. Y.; Ando, T.; Sawamoto, M. J. Am. Chem. Soc. 2003, 125, 5288–5289.
- (6) Mecerreyes, D.; Lee, V.; Hawker, C. J.; Hedrick, J. L.; Wursch, A.; Volsken, W.; Magbitang, T.; Huang, E.; Miller, R. D. *Adv. Mater.* 2001, 13, 204–208.
- (7) Blencowe, A.; Tan, J. F.; Goh, T. K.; Qiao, G. G. Polymer 2009, 50, 5–32.
- (8) Gao, H.; Matyjaszewski, K. Prog. Polym. Sci. 2009, 34, 317–350.
 (9) Wong, E. H. H.; Blencowe, A.; Qiao, G. G. Polym. Chem. 2013, 4, 4562–4565.
- (10) Ren, J. M.; Fu, Q.; Blencowe, A.; Qiao, G. G. ACS Macro Lett. 2012, 1, 681-686.
- (11) Rao, J. P.; Geckeler, K. E. Prog. Polym. Sci. 2011, 36, 887-913.
- (12) Altintas, O.; Lejeune, E.; Gerstel, P.; Barner-Kowollik, C. Polym. Chem. 2012, 3, 640.
- (13) Altintas, O.; Gerstel, P.; Dingenouts, N.; Barner-Kowollik, C. Chem. Commun. 2010, 46, 6291.
- (14) Aiertza, M. K.; Odriozola, I.; Cabanero, G.; Grande, H.-J.; Loinaz, I. Cell. Mol. Life Sci. 2012, 69, 337–346.
- (15) Altintas, O.; Barner-Kowollik, C. Macromol. Rapid Commun. 2012, 33, 958-971.
- (16) Ouchi, M.; Badi, N.; Lutz, J.-F.; Sawamoto, M. Nat. Chem. 2011, 3, 917–924.
- (17) Forster, E. J.; Berda, E. B.; Meijer, E. W. J. Am. Chem. Soc. 2009, 131, 6964–6966.
- (18) Jiang, J.; Thayumanavan, S. *Macromolecules* **2005**, *38*, 5886–5891.
- (19) Mes, T.; van der Weegen, R.; Palmans, A. R. A.; Meijer, E. W. Angew. Chem., Int. Ed. 2011, 50, 5085-5089.
- (20) Cherian, A. E.; Sun, F. C.; Sheiko, S. S.; Coates, G. W. J. Am. Chem. Soc. 2007, 129, 11350–11351.
- (21) Appel, E. A.; Dyson, J.; del Barrio, J.; Walsh, Z.; Scherman, O. A. Angew. Chem., Int. Ed. **2012**, *51*, 4185–4189.
- (22) Murray, B. S.; Fulton, D. A. Macromolecules 2011, 44, 7242–7252.
- (23) Tuten, B. T.; Chao, D.; Lyon, C. K.; Berda, E. B. Polym. Chem. 2012, 3, 3068-3071.
- (24) Gillisen, M. A. J.; Voets, I. K.; Meijer, E. W.; Palmans, A. R. A. Polym. Chem. 2012, 3, 3166–3174.
- (25) Perez-Baena, I.; Barroso-Bujans, F.; Gasser, U.; Arbe, A.; Moreno, A. J.; Colmenero, J.; Pomposo, J. A. ACS Macro Lett. **2013**, *2*, 775–779.
- (26) Dirlam, P. T.; Kim, H. J.; Arrington, K. J.; Chung, W. J.; Sahoo, R.; Hill, L. J.; Costanzo, P. J.; Theato, P.; Char, K.; Pyun, J. *Polym. Chem.* **2013**, *4*, 3765–3773.
- (27) Altintas, O.; Willenbacher, J.; Wuest, K. N. R.; Oehlenschlaeger, K. K.; Krolla-Sidenstein, P.; Gliemann, H.; Barner-Kowollik, C. *Macromolecules* **2013**, *46*, 8092–8101.
- (28) Adkins, C. T.; Muchalski, H.; Harth, E. Macromolecules 2009, 42, 5786–5792.
- (29) Goodman, C. M.; Choi, S.; Shandler, S.; DeGrado, W. F. Nat. Chem. Biol. 2007, 3, 252–262.
- (30) Wohlfart, S.; Gelperina, S.; Kreuter, J. J. Controlled Release 2012, 161, 264–273.
- (31) (a) Nederberg, F.; Connor, E. F.; Möller, M.; Glauser, T.; Hedrick, J. L. *Angew. Chem., Int. Ed.* **2001**, 40, 2712–2715. (b) Connor, E. F.; Nyce, G. W.; Myers, M.; Mock, A.; Hedrick, J. L. *J. Am. Chem. Soc.* **2002**, 124, 914–915. (c) Nyce, G. W.; Glauser, T.; Connor, E. F.;

Mock, A.; Waymouth, R. M.; Hedrick, J. L. J. Am. Chem. Soc. 2003, 125, 3046–3056. (d) Dove, A. P.; Pratt, R. C.; Lohmeijer, B. G. G.; Waymouth, R. M.; Hedrick, J. L. J. Am. Chem. Soc. 2005, 127, 13798–13799. (e) Pratt, R. C.; Lohmeijer, B. G. G.; Long, D. A.; Waymouth, R. M.; Hedrick, J. L. J. Am. Chem. Soc. 2006, 128, 4556–4557.

(32) Dove, A. P. ACS Macro Lett. 2012, 1, 1409-1412.

(33) Mecerreyes, D.; Humes, J.; Miller, R. D.; Hedrick, J. L.; Detrembleur, C.; Lecomte, P.; Jerome, R.; San Roman, J. Macromol. Rapid Commun. **2000**, *21*, 779–784.

(34) (a) Moad, G.; Rizzardo, E.; Thang, S. H. Aust. J. Chem. 2005, 58, 379–410. (b) Moad, G.; Rizzardo, E.; Thang, S. H. Aust. J. Chem. 2009, 62, 1402–1472.